

Carbon three-dimensional architecture formed by intersectional collision of graphene patches

Takazumi Kawai,^{1,*} Susumu Okada,² Yoshiyuki Miyamoto,¹ and Atsushi Oshiyama²

¹*Fundamental and Environmental Research Laboratories, NEC Corporation, 34 Miyukigaoka, Tsukuba 305-8501, Japan*

²*Institute of Physics and Center for Computational Science, University of Tsukuba, Tennodai, Tsukuba 305-8571, Japan*

(Received 22 March 2005; published 11 July 2005)

Graphite is the most stable form of carbon under room temperature and atmospheric pressure, and consists of two-dimensional honeycomb lattices with intralayer sp^2 bonding and rather weak van der Waals like interlayer interaction. When we supply gaseous small carbonic molecules such as methane to a patch of graphene, the patch will grow into graphite. Now, let us imagine a slightly different situation. Is a layered structure of graphite always formed, when we supply not methane molecules but another graphene patch? The answer from our computer simulations is “No.” Some graphene patches collide in parallel, but others at right angles, which result in a formation of junction structures (graphitic Y junctions). These junction structures are different from those of common sense for graphitic materials. Performing density functional calculations, we found that the reaction barrier height required for the formation of graphitic Y junctions are almost zero, and the binding energies per bond for each structure are ~ 1 eV. Furthermore, tight-binding molecular dynamics simulations showed high thermal stability and high formation probabilities for these junction structures. As applications of graphitic Y junctions, we will present two interesting structures, where we focus on the magnetic properties of junction structures and nanotube T-junction structures which are different from conventional models. We expect that graphitic Y junctions might be hidden in graphitic soot and not characterized yet in experiment. 3D architectures constructed from those unit structures are expected to have various applications with lightweight, ferromagnet, high molecular storage and high thermal conductor.

DOI: [10.1103/PhysRevB.72.035428](https://doi.org/10.1103/PhysRevB.72.035428)

PACS number(s): 61.46.+w, 61.48.+c, 73.22.-f

I. INTRODUCTION

Graphite, diamond, fullerene, nanotube, peapod—so many carbon-based materials possess many potential abilities for future technologies.^{1–4} After discoveries of fullerenes and nanotubes, architectures consisting of sp^2 network are getting a lot of attention. The most fascinating properties are toughness due to tightly bonded σ network and interesting electronic behavior, which arises from π orbital networks. Then the exploration for new carbon sp^2 network architecture is a very important and interesting theme. In the same way, sp^3 bonding states of carbon, which can take fourfold 3D bondings also present important and interesting properties to carbon related materials. Then, an addition of a few fourfold carbon atoms to sp^2 network systems would bring out some different potential abilities of carbon materials.

Theoretical approaches to explore new carbon structures suggested new classes of graphitic materials,^{5–8} which were claimed to be energetically stable. All these 3D architectures are characterized by junction structures *A* and *B* as shown in Fig. 1 and planar graphitic networks. Therefore, such junction structures are expected to be essential components to construct various 3D architectures, which utilize the fascinating properties of graphitic networks. We here raise a new structure *C*, in the rightmost of Fig. 1, which was not seen in the past works.^{5–8} We refer to these junction structures with “Y” section, which mainly consist of graphitic networks, as “graphitic Y junction” (GYJ).

Of course, we have to wait for the experimental discovery to have clear evidence for the existence of such 3D structures, however, we can also examine it theoretically. In this paper, we will show computational investigations on the thermal stability, formation processes and formation prob-

abilities of GYJ structures. We also describe some new architectures consisting of GYJ structures as important components.

In the next section, we examine thermal stability of GYJ structures. Formation processes for GYJ structures using graphitic patches as a precursor are developed in Sec. III. The formation barrier heights for corresponding formation processes are also presented. In Sec. IV tight-binding molecular dynamics simulations for the GYJ formation are performed under various initial conditions to evaluate the formation probability depending on the initial conditions. Some possible applications of GYJ junction structures are presented in Sec. V, and conclusion is appeared in Sec. VI.

II. THERMAL STABILITY OF GYJ

The above-mentioned theoretical studies have performed total energy calculations of the architectures, which correspond to the structural stability at rather lower temperature, but not at higher temperature. Then, we examined thermal stability of several junction structures, including those shown in Fig. 1 *A*, *B*, and *C* within orthorhombic or hexagonal lattices using tight-binding molecular dynamics (TBMD) simulations^{9,10} under constant temperature,^{11,12} where each unit cell has 100 to 150 carbon atoms including 6 to 8 atoms at the junction. Over 100 ps of simulation time is applied to verify the thermal stability of the structures. We found that the structures *A*, *B*, and *C* are particularly stable under high temperature (~ 2000 K), but other tested junction structures were found to be unstable. The GYJ *A* in the hexagonal lattice and *B* in the orthorhombic lattice survive at around 2000 K. For GYJ *C*, vertical bonds along the junction [see

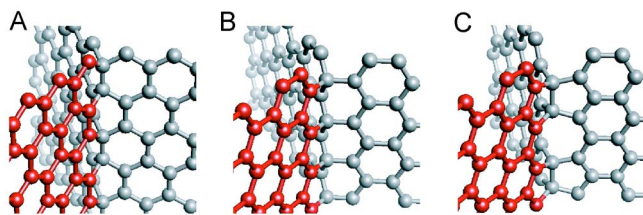


FIG. 1. (Color online) Schematic view of GYJ A, B, and C which are three-dimensional junction structures of sp^2 network, where red and gray spheres represent carbon atoms. Each structure can be divided into two graphene sheets, where one graphene sheet (red spheres) is attaching the armchair or zigzag edge to the surface of the other (gray spheres). For the GYJ C, the target graphene sheet has a line of defect array with 5–8 membered rings.

Fig. 1] are broken and recombine repeatedly. However, the junction structure is not broken even over 2000 K.

Then, we consider that these three GYJ structures are the most important and feasible structures as constituent units of various graphitic 3D architectures. To obtain further confirmation for the existence of such architectures in real materials, we need to discuss formation processes of these GYJ structures.

III. FORMATION PROCESS OF GYJ

A. Geometrical conditions

We recently proposed a new formation process based on the collision of graphene patches.⁹ Our simulations showed that rectangle graphene patches with the same size collided *in parallel* coalesced into nanotube, nanohorn and fullerene-like cage structures. Here the graphene patches have no edge terminations and have dangling bonds. We expected that such reaction procedures would be realized in high-temperature environment, which are indeed realized using laser ablation or arc discharge method.¹³

Our question is as to whether graphene patches colliding *at right angles* can form the GYJ structures. Focusing an attention to the continuity of graphitic network of six membered rings at the junction, one may find that the GYJ structures consist of two graphene sheets attaching armchair/zigzag edge of one sheet (red spheres in Fig. 1) to the surface of the other (gray spheres in Fig. 1). Note that some atoms of the target graphene surface, which originally make threefold planar network, take fourfold 3D bonding to combine two graphene sheets. For the formation of the GYJ C we need to introduce an array of 5 and 8 membered ring defects on a target (see Fig. 1). Here, the cohesive energy of a 5–8 defect array in a graphene sheet per unit cell is 3.0 eV higher than that of original graphene sheet, which is, however, lower than that of a Stone-Wales defect (~ 6.3 eV). By TBMD simulations, Nardelli *et al.* showed that the 5–8 defect is formed by the uniaxial strain on carbon nanotube,¹⁴ and we thus expect that a short array of 5–8 defects would be formed under a high temperature condition.

Therefore, the collision of graphene patches is one of the possible candidates for the formation of these GYJ structures. The next problem is as to whether the activation barriers for the formation are low enough.

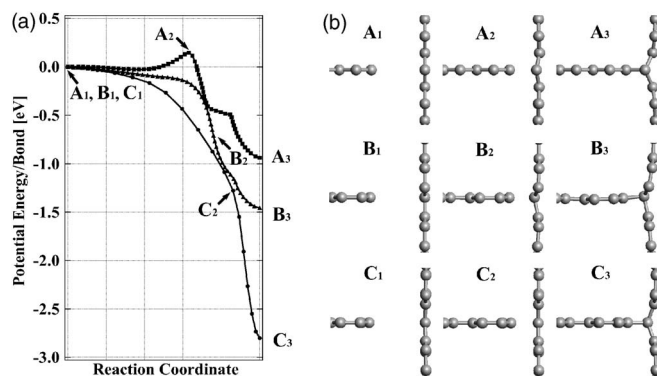


FIG. 2. (a) The potential energy curves for GYJ A (rectangles), B (triangles), and C (circles) formation as a function of reaction coordinate. The reaction coordinate is normalized by the length along the minimum energy path in the configuration space. The origin of potential energy is taken as that of initial configuration. (b) The cross-sectional views of atomic structures correspond to the formation steps indicated by the arrows in Fig. 2(a).

B. GYJ formation barrier height

To estimate the formation paths and barrier heights we used nudged elastic band method (NEBM).¹⁵ In the transition state theory, the activation barrier is defined as the highest energy point along the lowest energy path connecting two metastable atomistic configurations in the configurational energy landscape. In this context, the NEBM generates reliable reaction paths in chemical reactions involving complex rearrangement of atoms. The total energy calculations are performed by using the code of the conjugate-gradient method for diagonalization,¹⁶ which was successfully used for graphene ribbons.¹⁷ These calculations are based on the density functional theory (DFT) with norm-conserving pseudopotentials for electron-ion interaction and with local density approximation (LDA) for exchange-correlation energy.^{18–22} The valence wave functions are expanded in a plane-wave basis set with a cutoff energy of 60 Ry and integration over the Brillouin zone is carried out with four or five k points along the wave vector parallel to the junction axis. The coalescence of a termination-free graphene ribbon with armchair/zigzag edge and a graphene sheet without edge are simulated in the periodic boundary conditions with 42/24 carbon atoms per unit cell.

Figure 2 shows potential energy curves along the reaction paths for the formation of GYJ structures, and cross-sectional views of the atomic structure at each step indicated by the arrows. The origin of potential energy is taken as that of initial configurations where the distance between the edge and the surface is 4 Å. Surprisingly, there is no activation barrier for formation of junctions B and C with zigzag edge structure on the graphene ribbon. Although there is an activation barrier for the formation of GYJ A, it is not sufficiently large to disturb the junction formation (0.15 eV/bond) under a relatively high temperature condition in experiments. As for the formation of C type junction, the number of image between initial to final configuration is smaller than that of other calculations due to the computational restriction. It is, however, clear that there is no barrier

for the formation along the reaction path. Therefore, the GYJ structures would be formed independent of edge structures.

The formation process of the GYJ structures would be considered as follows: (1) Dangling bonds at the edge of graphene ribbon approach the surface of sp^2 network, and break the symmetry of π orbitals perpendicular to the graphene sheet surface. (2) The asymmetry induces electronic state transition of surface carbon atoms beneath the armchair/zigzag edge from sp^2 - to sp^3 -like state, and then the lattice at the junction is distorted gradually. (3) Finally, dangling bond states of sp^2 network and that from sp^3 -like states on the surface make covalent bonds between edge and the surface.

Why does an armchair edge need activation barrier, while a zigzag edge not? In the zigzag edges, the energy levels of the states coming from lacking of edge termination are at around the Fermi level. In other words, those states are rather reactive dangling bond states. Meanwhile, for the termination-free armchair edge, the corresponding edge-localized states are below the Fermi level for about 2 eV, which are relatively stable.¹⁷ Such a lower energy level is due to a formation of triple-bonding-like states at the armchair edge without termination. Then the coalescence of armchair edge and graphene surface needs the corresponding electronic states to be activated throughout the way of bringing the edge close to the surface, i.e., the procedure of coalescence involves an activation barrier. Nevertheless, the triple-bonding-like states at armchair edge should be more reactive than an acetylene molecule on graphene surface, because the reaction between the acetylene molecule and graphene sheet requires not only graphene surface but also linear $\text{H}-\text{C}\equiv\text{C}-\text{H}$ chain of the acetylene molecule to bend to form threefold bonding structure.

IV. MD SIMULATIONS FOR GYJ FORMATION

A. GYJ formations depending on initial configurations

To make sure the possibility of the GYJ formations, we also performed TBMD simulations of colliding graphene sheet and graphene ribbon without edge termination using various initial atomic configurations. Our unit cell has about 120 carbon atoms in the periodic boundary conditions. Simulations of reaction were performed with 600–1000 K of initial random velocities of each atom given by randomized numbers including 10–170 meV/atom of translational kinetic energy to collide graphene sheet and graphene ribbon. Since the change in translational kinetic energy to collide did not affect the results dramatically, simulations below were done with about 20 meV/atom of energy which is smaller than the energy corresponding to initial temperature.

Tight-binding MD simulations for collision of graphene ribbon with either armchair or zigzag edge and graphene sheet at right angles result in the formation of GYJs. The snapshots of the reaction process for the structure A formation are shown in Fig. 3(a). Several simulations showed that a lateral sliding of the colliding ribbon with respect to the target graphene surface rarely suppress the junction formation for coalescence at right angles [Fig. 3(b)] both for the formation of GYJ A and B. This is because the formations of

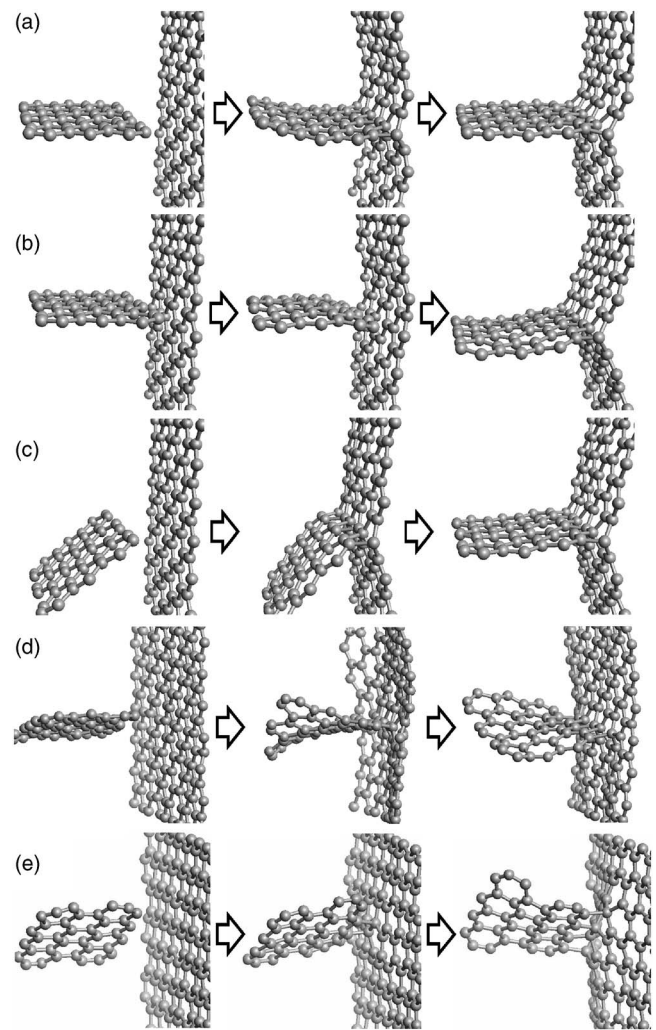


FIG. 3. Snapshots of molecular dynamics simulations for the formation of GYJ A from a collision of a graphene sheet and a graphitic ribbon (a) at right angles, (b) with 1 Å shift perpendicular to the ribbon surface, (c) with 40° tilt angle, and (d) with 15° of azimuthal angle rotation. (e) GYJ formation from the reaction of zigzag edge and graphene surface with 30° of azimuthal angle.

GYJ A and B need no special reaction sites on the graphene surface, and lines of reaction sites on the graphene sheet are aligned with 2–3 Å intervals. On the other hand, a line of 5–8 defects on the graphene sheet is required for the formation of GYJ C. Then a lateral sliding of the incident graphene ribbon sometimes disturbs the formation of GYJ C.

In usual experimental conditions, it would be difficult to control a tilt angle of an incident graphene ribbon, so we tested an influence of the tilt angle on the formation process. When the incident graphene ribbon was tilted 40° off from the right angle, the reactions often result in the formation of GYJ structure successfully. The snapshots in Fig. 3(c) show a simulation result for successful GYJ A formation with 40° of an initial tilt angle. When the tilt angle is beyond 60°, GYJ A and B are rarely formed and an incident graphene ribbon is often stacked on the target graphene sheet in parallel without any mutual covalent bonding, while the GYJ C are still formed successfully. We will come back to this point later.

An azimuthal angle of graphene sheet and ribbon is also an important factor for the reaction and depends on the edge structure due to necessity of commensurate matching. For simulations, we used a small graphene patch (42/36 atoms for armchair/zigzag edge reaction) in place of ribbon and changing the azimuthal angle. A little bit larger graphene sheet with 140, 128 and 136 carbon atoms are used for a target in the periodic boundary condition to form GYJ A, B and C, respectively. A simulation for the formation of GYJ A with 15° of azimuthal angle rotation is shown in Fig. 3(d), where the small patch with armchair reaction head found a stable reaction point at -15° of azimuthal angle rotation on the target graphene surface. The patch finally made connections of covalent bonds between graphene sheet by twisting itself, and form local GYJ A structure successfully. Due to the high reactivity of zigzag edge dangling bond with π electrons on graphene surface, the collisions of zigzag edge and graphene surface often make junction structure independent of whether the reactive edge and surface are commensurate or not along the resulting junction structure [Fig. 3(e)].

B. Formation probabilities for GYJ

For the analytical evaluation of the GYJ formation probability or sticking rate for a graphene patch on the graphene sheet, we focused on two important factors, i.e., tilt angle and azimuthal angle under two different initial given temperatures. We performed 20 times simulations per each tilt (azimuthal) angle of collision by changing the random numbers to generate the initial random velocities. Here, the formation of the GYJ structures is defined by the existence of more than four (two) bonds out of six (four) expected maximum bonds between armchair (zigzag) edge of a graphene patch and a graphene sheet after 2.4 psec simulation time. In our simulations, the randomized initial velocities cause a small lateral sliding or angular momentum of a colliding ribbon or a patch since there are some residual velocities which are not completely cancelled due to a small number of atoms. In other words, effects of lateral sliding and angular momentum are reflected in the resulting probabilities to some extent.

The formation probabilities as a function of tilt angle are shown in Fig. 4(a). When the range of tilt angle is up to 35° off from the right angle, more than half of the reactions reached to the Y-junction independent of the junction structures A, B and C. Low probabilities of GYJ C structure at smaller tilt angles are due to a lateral sliding of the patch, which brings the reaction head of ribbon to the different reaction sites from that of targeted GYJ C structure. The resulting junction structures are often identified as a GYJ B structure with adjacent 5–8 defects. By tilting the incident graphene ribbon, the formation probabilities of GYJ B structure are reduced to zero rather rapidly, i.e., the reaction between a zigzag edge of ribbon and a graphene surface becomes difficult for larger tilt angles. On the other hand, the reactivity between a zigzag edge and a 5–8 defect array does not largely depend on the tilting angle, and then, the incident ribbon is able to reach the 5–8 defect without reacting with other surface points. Then the formation probabilities of GYJ

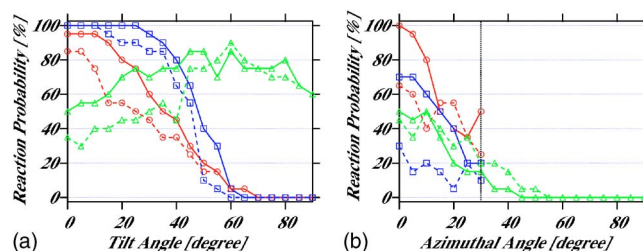


FIG. 4. (Color online) Formation probabilities for collisions of a graphene sheet and a graphitic ribbon or a patch as a function of (a) tilt angle and (b) azimuthal angle. Open circle (red lines), rectangle (blue lines), and triangle (green lines) represent formation probabilities for GYJ A, B, and C junctions, respectively. Solid and dotted lines correspond to 600 K and 1000 K of initial given temperatures.

C are kept almost constant for larger tilt angles. Above mentioned GYJ B with 5–8 defect array structure may be annealed to GYJ C, because GYJ C is energetically more stable than GYJ B with a 5–8 defect array. The annealing temperature, however, expected to be higher than 2000 K since these structures are stable at around 2000 K as described in Sec. II.

The azimuthal orientations of a graphene patch on the graphene sheet ranging from 0 to 30° are enough to test GYJ A and B formations if a small translational shift is allowed. Meanwhile, 0 to 90° of azimuthal orientations are required for the examinations of GYJ C formation. The formation probabilities as a function of azimuthal angles are shown in Fig. 4(b). Over half of the reactions for an armchair edge (a zigzag edge) of graphene patch and graphene sheet resulted in GYJ A (B) structures up to 15° of azimuthal angle rotation. Even for the azimuthal angle of 30° , more than 20% simulations succeeded to form GYJ A (B) structures.

It is interesting that a zigzag edge of graphene patch and a graphene sheet often form a junction structure as shown in Fig. 3(e) even when they fail to form GYJ B structure. Here, the zigzag edge is incommensurate with the graphene surface along this new junction structure, and then, the formation of the junction is limited to a short interval. When we just consider the reaction rate of zigzag edge and graphene surface and do not distinguish detailed atomic structure of junctions, the formation probabilities of junction structures are over 90% independent of its azimuthal angle rotation. Although the formation of GYJ C is a little bit lower than other structures, the formation probability of 15% at 30° of azimuthal angle rotation is not so low, when we consider the stability of GYJ structures. As a result, GYJ structures were formed rather easily if the formation processes are initiated by the graphene patch formation.

V. APPLICATIONS OF JUNCTION STRUCTURES

A. Magnetic properties of GYJ based structure

The electronic properties of GYJ based structures mostly depend on the width and the edge orientation of constituent graphene ribbons. The reason is that the electronic properties are determined by π electrons around the Fermi level whose networks are separated into graphite strips by carbon atoms

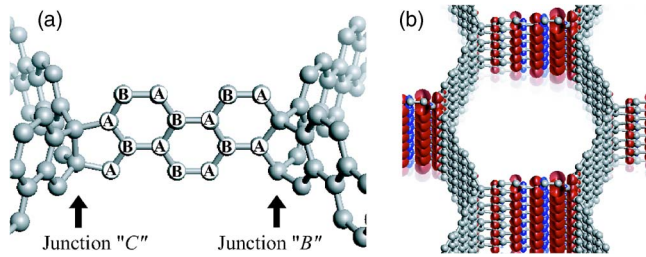


FIG. 5. (Color online) (a) The unit structure for a new 3D architecture formed of GYJ *B* and *C*. The letters on each sphere classify the “A” site and “B” site. (b) Total spin density isosurfaces of the new architecture. Red isosurfaces represent majority spins density, and blue ones minority.

at the junctions. Meanwhile, the σ states at the junction would not change those properties dramatically.

Here, we focus on the “edge state” on a graphene ribbon, which is one of the most interesting properties of sp^2 network architectures.^{23–26} In brief, the “edge state” appears upon termination of periodic boundary conditions of π -electron network by zigzag edge, and forms almost flat dispersion bands at the Fermi level. It has been suggested that the edge state induces ferromagnetic order of the spin along the edge.²³ Some groups in experiment interpret ferromagnetic order of their carbonaceous materials as a result coming from the edge state.²⁷ There are two atomic sites in its hexagonal primitive cell of graphite and all the atomic sites are classified into two sublattices “A” and “B” (bipartite lattice). General form of the ribbons with zigzag edge has the same number of “A” sites and “B” sites on AB bipartite lattice, and total spin number is equal to zero, so there is no magnetism in macroscopic properties.²⁸ However, some particular edge structures can make disproportion between numbers of “A” sites and “B” sites. A new architecture is built up with the combination of the structures *B* and *C*, where one of the graphitic strips has both a Klein type edge and a zigzag edge^{29,30} as shown in Fig. 5(a).

The electronic structure of the GYJ in Fig. 5(a) is calculated using local-spin-density-functional method with *ab initio* pseudopotentials^{25,26} and shows a band splitting at the Fermi level. The number of total spin in this system is 1.3 per unit cell. Figure 5(b) shows isosurface of total spin density. The spin distribution is similar to that of the graphene ribbon with two different types of termination,³⁰ although weak interaction between π electrons of different graphene planes at the junction changes the original flat band into dispersive one crossing the Fermi level, which reduces the total spin polarization from ideal value of 2.0. The energy gain for spin polarization is 0.11 eV per unit cell (50 carbon atoms). Although it might be difficult to form the long sequence of the new architecture, we expect that a few nanometers of the sequence would be enough to reveal the specific spin polarization.²⁴

B. Nanotube T junctions

Recently, the Y and T junctions of nanotubes have attracted current research interest as new nanoscale devices.³¹

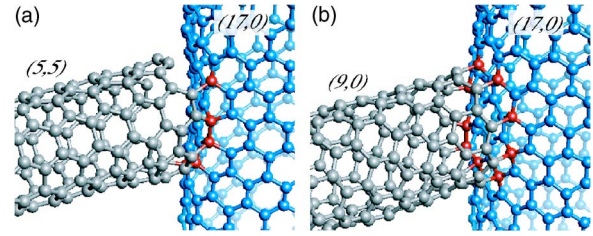


FIG. 6. (Color online) Resulting structures for the coalescence of nanotubes (17,0) sidewall (blue spheres) with termination free (a) (5,5) edge and (b) (9,0) edge (gray spheres). Fourfold atoms at the junction, which originally belong to the (17,0) nanotube, are indicated by the red spheres.

The formation processes of GYJ are applicable to a coalescence of two nanotubes resulting in a T junction, where a termination-free open end of a nanotube collides with a sidewall of the other nanotubes. For the junction formation of nanotube, there is some amount of curvature at the target and incident edge structure. However, these effects would not be crucial for the junction formation using the nanotubes with large diameter, where the local curvature is not so large. The atomic structures of the resulting nanotube T junctions are significantly different from the conventional nanotube T-junction models.

We performed the coalescence of zigzag (17,0) nanotube with armchair (5,5) or zigzag (9,0) nanotube to form nanotube T-junction structure using TBMD simulations. The zigzag (17,0) nanotube consists of 476 atoms in the periodic boundary condition and the open end (5,5) and (9,0) nanotubes consist of 160 and 162 atoms, respectively. The initial random velocities which correspond to the temperature of 500 K including ~ 2 meV/atom of a small translational velocity to collide nanotubes are given using random numbers. The resulting structures are shown in Fig. 6. Due to the high azimuthal-angle dependency of armchair edge as shown in Fig. 4(b), only partial bond formations along the edge [Fig. 6(a)] are allowed in the simulation. For the coalescence of zigzag (9,0) and (17,0) nanotubes, all the bonds are formed along the zigzag edge. We performed simulations using 5 sets of different initial randomized velocities for each (5,5) with (17,0) nanotube, and (9,0) with (17,0) nanotube to coalesce. Almost all the simulations indicate a similar tendency as described above. We expect that the nanotube with larger diameter will form the junction easily even for armchair nanotubes.

The nanotube T junction formed here uses sp^3 -like fourfold bondings at the junction, which is indicated by the red spheres in Figs. 6(a) and 6(b), while the conventional nanotube T junctions are expected to consist of only sp^2 -like threefold bonding network.³² Thus the inner space of present T junction is separated by the sidewall of original nanotube, while conventional ones have continuous inner space. One of the most important procedures to construct a nanotube T junction, here, is extraction of impurities at the nanotube end to obtain a termination-free open end of nanotube. The termination free edge of nanotube end would be prepared by the irradiation of appropriate electron beam experimentally. Our results indicate a possibility for intentional formation of

nanotube T-junction structures or electrical circuits by single wall carbon nanotube. For multiwall nanotubes, the formation of these junction structures might be difficult because reactive termination free edges form interwall bonding connections by lip-lip interaction, and are inactivated readily.^{33,34}

VI. CONCLUSION

We investigated thermal stability and a formation process of GYJ structures, which is a coalescence of a graphene sheet at the edge and a surface of the other. We found that the formation barrier for the GYJ *A* is significantly low (~ 0.15 eV/bond) and there is no barrier for the formation of GYJ *B* and *C*. We also performed TBMD simulations to evaluate the probability of the junction formation by colliding the graphene ribbon or patch and graphene sheet. The formation probabilities are more than 50% up to 35° of tilt angle from the right angle for every GYJ structure. The azimuthal angle dependency is also investigated using a small graphene patch in place of graphene ribbon. For up to 30° of azimuthal angle rotation, the formation probabilities are over 15%. We expect that these probabilities are high enough to realize GYJ structures in some experiments, since these junctions are not broken even over 2000 K of high temperature from constant temperature TBMD simulations.

We assume that random combinations of these junction structures are already realized in some real materials that mainly consist of sp^2 network, e.g., nanohorn that is a hedgehog-like carbon allotrope.³⁵ Because the core part of nanohorn structure is thermally stable and never dissociated from each other in some solutions, sp^2 networks would be connected with each other not with weak interlayer interac-

tion but with covalent bonds. Using ^{13}C -NMR technique, Imai *et al.* showed that majority part of carbon nanohorn structure at the core consists of rather flat sp^2 network.³⁶ The results suggest that curved sp^2 networks using five- or seven-membered rings would not be applied to the nanohorn core structure. We also consider that such curved structures would be energetically unfavorable due to large curvature inside nanohorn compared to GYJ structures.

Therefore, composite of GYJ structures is one of possible candidates for nanohorn core structure, while it is very difficult to determine its atomic structure in experiments due to immense complexity of the architecture. The first step to know the atomic scale structure of carbon nanohorn would be to verify the existence of the minority sp^3 bondings and the precise sp^2/sp^3 ratio at the core. With the above facts and present results for spin polarizations, we consider that development of synthesis and purification process may produce magnetic nanohorns selectively.

Utilizing GYJ formation process as a glue to connect nanocarbon structures, further various three-dimensional architectures would be realized. In an analogy of graphitic materials, it is also expected that architectures constructed from GYJ structures are applicable to molecular storage due to large surface area, heat sink material with high thermal conductivity.

ACKNOWLEDGMENTS

Part of the calculations were performed on the SX5 Supercomputer System at the NEC Fuchu Plant. This work was in part performed under the management of Nano Carbon Technology project supported by NEDO, Nanotechnology Materials Program (NEDO) and ACT-JST (Japan Science and Technology Corporation).

*Corresponding author. Email address: t-kawai@da.jp.nec.com

¹W. E. Pickett, Phys. Rev. Lett. **73**, 1664 (1994).

²A. Modi, N. Koratkar, E. Lass, B. Wei, and P. M. Ajayan, Nature (London) **424**, 171 (2003).

³A. M. Fennimore, T. D. Yuzvinsky, W.-Q. Han, M. S. Fuhrer, J. Cumings, and A. Zettl, Nature (London) **424**, 408 (2003).

⁴A. Javey, J. Guo, Q. Wang, M. Lundstrom, and H. Dai, Nature (London) **424**, 654 (2003).

⁵H. R. Karfunkel and T. Dressler, J. Am. Chem. Soc. **114**, 2285 (1992).

⁶A. T. Balaban, D. J. Klein, and C. A. Folden, Chem. Phys. Lett. **217**, 266 (1994).

⁷N. Park and J. Ihm, Phys. Rev. B **62**, 7614 (2000).

⁸K. Umemoto, S. Saito, S. Berber, and D. Tomanek, Phys. Rev. B **64**, 193409 (2001).

⁹T. Kawai, Y. Miyamoto, O. Sugino, and Y. Koga, Phys. Rev. B **66**, 033404 (2002).

¹⁰C. H. Xu, C. Z. Wang, C. T. Chan, and K. M. Ho, J. Phys.: Condens. Matter **4**, 6047 (1992).

¹¹S. Nosé, J. Chem. Phys. **81**, 511 (1984).

¹²W. G. Hoover, Phys. Rev. A **31**, 1695 (1985).

¹³F. Kokai, A. Koshio, K. Hirahara, K. Takahashi, A. Nakayama,

M. Ishihara, Y. Koga, and S. Iijima, Carbon **42**, 2515 (2004).

¹⁴M. Buongiorno Nardelli, B. I. Yakobson, and J. Bernholc, Phys. Rev. B **57**, R4277 (1998).

¹⁵H. Jonsson, G. Mills, and K. W. Jacobsen, in *Classical and Quantum Dynamics in Condensed Phase Simulations*, edited by B. J. Berne, G. Ciccotti and D. F. Coker (World Scientific, Singapore, 1998).

¹⁶O. Sugino and A. Oshiyama, Phys. Rev. Lett. **68**, 1858 (1992).

¹⁷T. Kawai, Y. Miyamoto, O. Sugino, and Y. Koga, Phys. Rev. B **62**, R16349 (2000).

¹⁸P. Hohenberg and W. Kohn, Phys. Rev. **136**, B864 (1964).

¹⁹W. Kohn and L. Sham, Phys. Rev. **140**, A1133 (1965).

²⁰D. M. Ceperley and B. J. Alder, Phys. Rev. Lett. **45**, 566 (1980).

²¹J. P. Perdew and A. Zunger, Phys. Rev. B **23**, 5048 (1981).

²²N. Troullier and J. L. Martins, Phys. Rev. B **43**, 1993 (1991).

²³M. Fujita, K. Wakabayashi, K. Nakada, and K. Kusakabe, J. Phys. Soc. Jpn. **65**, 1920 (1996).

²⁴K. Nakada, M. Fujita, G. Dresselhaus, and M. S. Dresselhaus, Phys. Rev. B **54**, 17954 (1996).

²⁵S. Okada and A. Oshiyama, Phys. Rev. Lett. **87**, 146803 (2001).

²⁶S. Okada and A. Oshiyama, J. Phys. Soc. Jpn. **72**, 1510 (2003).

²⁷P. Esquinazi, D. Spemann, R. Hohne, A. Setzer, K.-H. Han, and

- T. Butz, Phys. Rev. Lett. **91**, 227201 (2003).
- ²⁸E. H. Lieb, Phys. Rev. Lett. **62**, 1201 (1989).
- ²⁹D. J. Klein and L. Bytautas, J. Phys. Chem. A **103**, 4196 (1999).
- ³⁰K. Kusakabe and M. Maruyama, Phys. Rev. B **67**, 092406 (2003).
- ³¹M. Terrones, F. Banhart, N. Grobert, J.-C. Charlier, H. Terrones, and P. M. Ajayan, Phys. Rev. Lett. **89**, 075505 (2002).
- ³²M. Menon, A. N. Andriotis, D. Srivastava, I. Ponomareva, and L. A. Chernozatonskii, Phys. Rev. Lett. **91**, 145501 (2003).
- ³³Y.-K. Kwon, Y. H. Lee, S.-G. Kim, P. Jund, D. Tománek, and R. E. Smalley, Phys. Rev. Lett. **79**, 2065 (1997).
- ³⁴M. Buongiorno Nardelli, C. Brabec, A. Maiti, C. Roland, and J. Bernholc, Phys. Rev. Lett. **80**, 313 (1998).
- ³⁵S. Iijima, M. Yudasaka, R. Yamada, S. Bandow, K. Suenaga, and F. Kokai, Chem. Phys. Lett. **309**, 165 (1999).
- ³⁶H. Imai, P. K. Babu, E. Oldfield, A. Wieckowski, D. Kasuya, T. Azami, Y. Shimakawa, M. Yudasaka, Y. Kubo, and S. Iijima (in preparation).